Available online at www.sciencedirect.com
SCIENCE DIRECT®
PERGAMON
Electrochimica Acta 48 (2003) 2589–2592
ELECTROCHIMICA Acta
www.elsevier.com/locate/electacta

Electrochemical properties and structural characterization of layered $Li[Ni_{0.5}Mn_{0.5}]O_2$ cathode materials

Y.-K. Sun [a,*], C.S. Yoon [b], Y.S. Lee [c]

[a] Department of Chemical Engineering, Center for Information and Communication Materials, Hanyang University, 17 Haendang-Dong, Seongdong-Gu, Seoul 133-791, South Korea
[b] Department of Materials Science and Engineering, Hanyang University, Seongdong-Gu, Seoul 133-791, South Korea
[c] High-Tech Research Center, Kanagawa University, Yokohama 221-8686, Japan

Received 27 January 2003; received in revised form 4 April 2003; accepted 7 April 2003

Abstract

Layered $Li[Ni_{0.5}Mn_{0.5}]O_2$ materials with high homogeneity and crystallinity were prepared using high speed ball milling. The $Li[Ni_{0.5}Mn_{0.5}]O_2$ electrode delivered a high discharge capacity of 152 mA h g^{-1} between 2.8 and 4.3 V with excellent cycleability. The TEM analysis showed that the $Li[Ni_{0.5}Mn_{0.5}]O_2$ electrode went through a considerable morphological change without altering its initial layered structure while the electrode retained its initial discharge capacity even after 50 cycles.

Keywords: Lithium secondary batteries; Layered manganese; Cathode materials; Structural change; TEM

1. Introduction

In the last 10 years, various lithiated transition metal oxides have been synthesized and investigated as alternative cathode materials for secondary lithium secondary batteries to replace the widely used $LiCoO_2$ material. Obviously, $LiCoO_2$ is an excellent cathode material with good capacity, reversibility and rate capability, but suffers from the high cost and relatively toxicity of cobalt. Therefore, the research in this area has focused mainly on $LiMn_2O_4$ and $LiMO_2$ (M = Ni and Mn) compounds [1–3]. $LiMn_2O_4$ has a smaller capacity compared with $LiCoO_2$, and a poor cycling behavior at elevated temperatures, e.g. at 55 °C [4,5]. $LiNiO_2$ has been one of the most attractive material because of its low cost and larger capacity compared with $LiCoO_2$. However, $LiNiO_2$ has severe problems associated with preparing phase-pure material, the poor electrochemical performance, and thermal instability in organic electrolytes in charged state [6]. As an alternative Li–Mn–O material to the spinel $LiMn_2O_4$, the layered $LiMnO_2$ structure has been actively studied due to its high theoretical discharge capacity of 285 mA h g^{-1} [7–9]. $LiMnO_2$ was observed to undergo a detrimental phase transformation to a spinel-like phase through minor atomic rearrangements during the first removal and subsequent cycling of Li, leading to eventual degradation of electrode performance [10,11]. Recently, a concept of a one-to-one solid state mixture of $LiNiO_2$ and $LiMnO_2$, i.e. $Li[Ni_{0.5}Mn_{0.5}]O_2$, was adopted by Ohzuku and Makimura [12] to overcome the disadvantages of both $LiNiO_2$ and $LiMnO_2$.

In this paper, a layered $Li[Ni_{0.5}Mn_{0.5}]O_2$ material was prepared using the solid-state reaction method and its electrochemical properties in conjunction with the microstructural changes during electrochemical cycling were studied.

2. Experimental

$LiOH \cdot H_2O$ (Aldrich Chemical Co.), $Ni(OH)_2$ (Junsei Chemical Co.) and γ-MnOOH (Sedema Chemical Co.) were used as the precursor materials. $Li[Ni_{0.5}Mn_{0.5}]O_2$ powders were prepared by solid-state reaction method using a 8005 zirconia ceramic vial set. Stoichiometric

* Corresponding author. Tel.: +82-2-2290-0524; fax: +82-2-2282-7329.
E-mail address: yksun@hanyang.ac.kr (Y.-K. Sun).

0013-4686/03/$ - see front matter © 2003 Elsevier Science Ltd. All rights reserved.
doi:10.1016/S0013-4686(03)00301-3

amounts of $Ni(OH)_2$ and MnOOH were placed in the zirconia vial with zirconia balls and mixed for 1 h using on a Spex 8000M Mixer/Mill after which pellets were pressed from the powder. The pellets were heated at 600 °C in air for 48 h and ground in a agate mortar. The ground powder was mixed with the appropriate amount of $LiOH \cdot H_2O$ in the zirconia ceramic vial set for 1 h. The powders were pressed again, and heated at 950 °C for 20 h in air, and then quenched to room temperature.

Powder X-ray diffractions (Rigaku, Rint-2000) using CuKα radiation was used to identify the crystalline phase of the as-prepared powders. Structure of the powder before and after cycling was also observed using transmission electron microscopy (TEM, JEOL 2010). Charge–discharge cycles were performed in CR2032 coin type cells. The cell consisted of a cathode and a lithium metal anode separated by a porous polypropylene film. For the fabrication of the electrode, the mixture, which contained 20 mg of $Li[Ni_{0.5}Mn_{0.5}]O_2$ powders and 12 mg conducting binder (8 mg of teflonized acetylene black (TAB) and 4 mg of graphite), was pressed on a 2.0 cm^2 stainless screen at 500 kg cm^{-2}. The electrolyte was a 1:2 mixture of ethylene carbonate (EC) and dimethyl carbonate (DMC) containing 1 M $LiPF_6$ by volume.

3. Result and discussion

Fig. 1 shows the X-ray diffraction pattern of $Li[Ni_{0.5}Mn_{0.5}]O_2$ powder with the Miller indices indicated. All of the peaks were indexed based on the space group, $R3m$. Judging from the XRD pattern alone, the as-prepared powders were composed of a single phase with the layered $LiMnO_2$ structure and the diffraction peaks, in general, were quite narrow indicating a good crystallinity of the prepared material. The peaks between 20 and 25° in Fig. 1 were generated by superlattice ordering of the transition metals in the 3a site, indicating a layered structure with the Li_2MnO_3 character [13]. The lattice constants, a and c, of the as-prepared $Li[Ni_{0.5}Mn_{0.5}]O_2$ were 2.887 and 14.262 Å, respectively. The measured c/a ratio of $Li[Ni_{0.5}Mn_{0.5}]O_2$ is 4.96, which closely matches the values from ideal hexagonal structure (4.96–4.97).

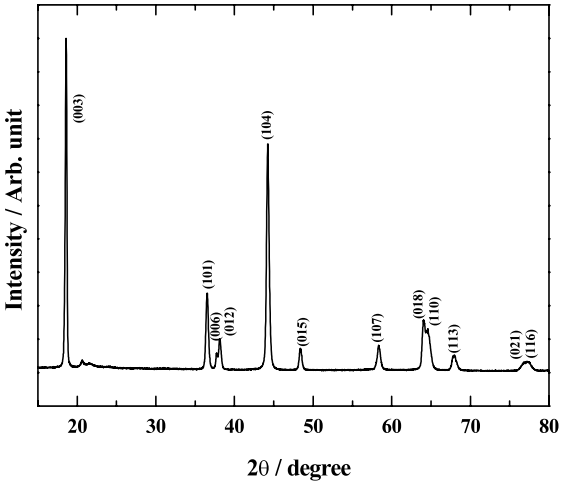

Fig. 1. X-ray diffraction pattern of the as-prepared $Li[Ni_{0.5}Mn_{0.5}]O_2$ powder.

Fig. 2 shows the charge–discharge curves for the Li/$Li[Ni_{0.5}Mn_{0.5}]O_2$ cell as a function of cycle number between 2.8 and 4.3 V at a constant current density of 0.1 mA cm^{-2} (10 mA g^{-1}) and 30 °C. The $Li[Ni_{0.5}Mn_{0.5}]O_2$ electrode delivers an initial discharge capacity of 152 mA h g^{-1} and shows excellent cycleability without any capacity loss after 50 cycles. It is also observed that their charge–discharge curves do not change even after 50 cycles.

The charge–discharge curves of the Li/$Li[Ni_{0.5}Mn_{0.5}]O_2$ cell cycled in different voltage ranges are shown in Fig. 3(a); corresponding discharge capacities are shown in Fig. 3(b). The electrochemical cycles were carried out at a constant current density of 0.1 mA cm^{-2} (10 mA g^{-1}) at 30 °C. The Li/$Li[Ni_{0.5}Mn_{0.5}]O_2$ cell had very smooth and monotonous voltage profiles, closely resembling the voltage profile reported by other researchers [12,13]. It is noted that the charge–discharge curves did not change even after increasing upper cut-off voltage to 4.6 V. The discharge capacity increased linearly with the upper cut-off voltage limit. In the 2.8–4.3 V voltage range, the discharge capacities of the $Li[Ni_{0.5}Mn_{0.5}]O_2$ electrode remained around 150 mA h g^{-1} during cycling. Upon increasing the upper cut-off voltage to 4.6 V, the measured discharge capacity rose to 190 mA h g^{-1} with no observable capacity loss during cycling.

In Fig. 4 is the XRD pattern obtained from the $Li[Ni_{0.5}Mn_{0.5}]O_2$ electrode after 50 cycles at 2.8 and 4.3 V. Comparing the XRD patterns in Figs. 1 and 4, no significant structural change was observed after electrochemically. TEM characterization, however, showed that the $Li[Ni_{0.5}Mn_{0.5}]O_2$ powders underwent a con-

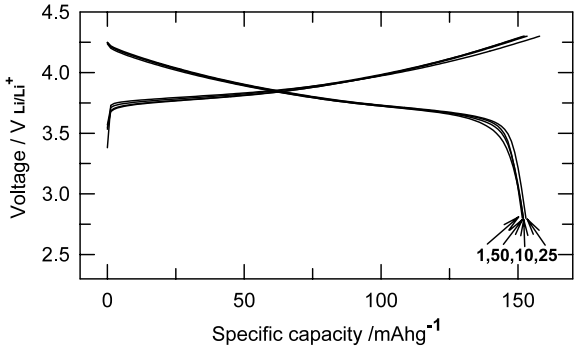

Fig. 2. Charge–discharge curves of the Li/$Li[Ni_{0.5}Mn_{0.5}]O_2$ cell at a current density of 0.1 mA cm^{-2} (10 mA g^{-1}) between 2.8 and 4.3 V at 30 °C.

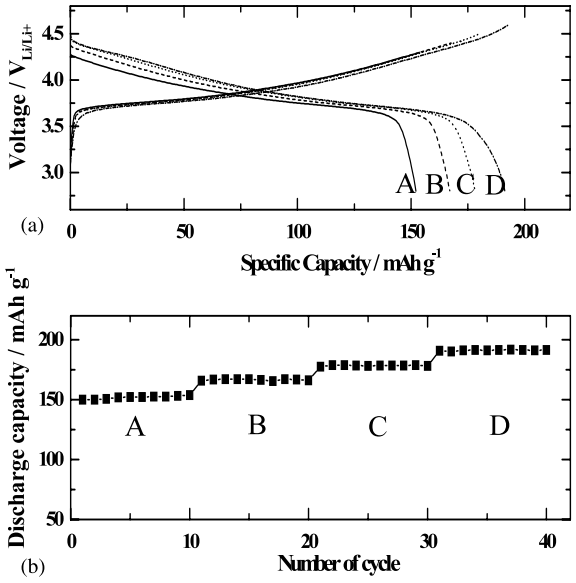

Fig. 3. (a) Charge–discharge curves of Li/Li[$Ni_{0.5}Mn_{0.5}$]O_2 cells in different voltage ranges at a current density of 0.1 mA cm^{-2} (10 mA g^{-1}) at 30 °C. (b) Specific discharge capacity of Li/Li[$Ni_{0.5}Mn_{0.5}$]O_2 cell as a function of number of cycle.: A, 2.8–4.3 V; B, 2.8–4.4 V; C, 2.8–4.5 V; D, 2.8–4.6 V.

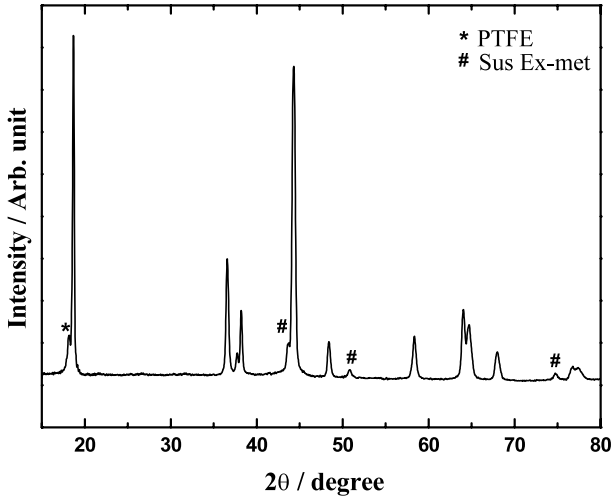

Fig. 4. X-ray diffraction patterns of the Li[$Ni_{0.5}Mn_{0.5}$]O_2 electrode after cycled at a current density of 0.1 mA cm^{-2} (10 mA g^{-1}) between 2.8 and 4.3 V at 30 °C.

siderable morphological change after electrochemical cycling in spite of the structural stability observed with XRD. Shown in Fig. 5 are the bright field TEM image and electron diffraction pattern of the as-prepared Li[$Ni_{0.5}Mn_{0.5}$]O_2 powders. Even though the XRD pattern in Fig. 1 indicated the as-prepared powders were a single phase with the layered structure, Fig. 5(a) shows that the as-prepared powders mostly consisted of uniformly sized particles (below 100 nm) with the rhomobohedral structure intermixed with 300–400 nm sized particles belonging to the spinel structure (confirmed with the single crystal electron diffraction). Since

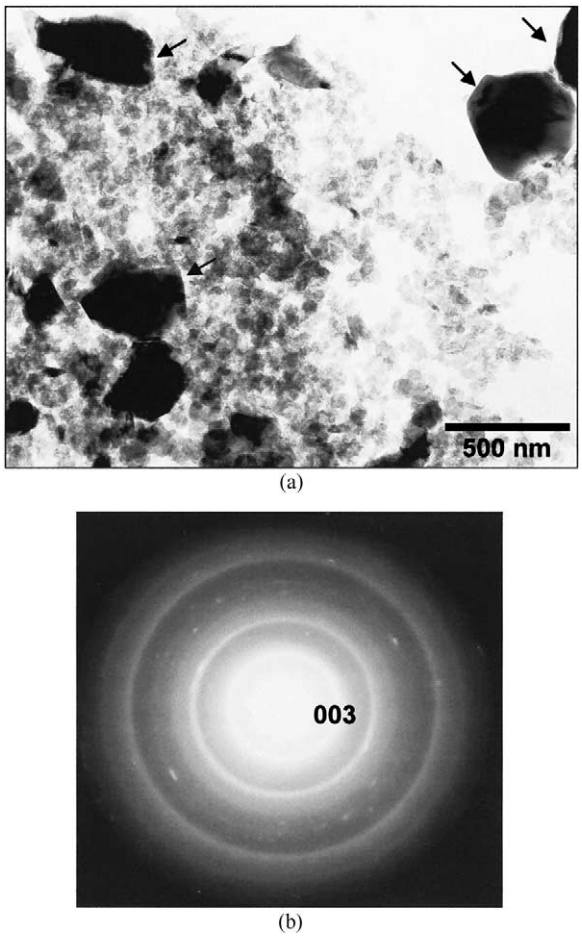

Fig. 5. (a) Bright field TEM image of the as-prepared Li[$Ni_{0.5}Mn_{0.5}$]O_2 powders (spinel particles are indicated by arrows); (b) electron diffraction pattern from the 100 nm sized particles.

volume fraction of the spinel structure was comparatively small, we expect the spinel particles to have little bearing on the electrochemical properties of the as-prepared powders. In Fig. 5(b) is the electron diffraction pattern from the smaller particles, which matched the XRD pattern in Fig. 1 quite well in both intensities and peak locations, suggesting that the as-prepared material indeed had the rhombohedral structure.

TEM image of the cycled electrode in Fig. 6(a) was strikingly different from Fig. 5(a). The 100 nm sized particles could no longer be observed in the cycled electrode; instead, the particles were converted into much larger particles whose ranged up to 500–600 nm. Using the selected area diffraction, crystallographic structure of these large particles were confirmed to belong to the rhombohedral structure in agreement with the XRD data in Fig. 4. A representative single crystal diffraction pattern in 110 zone of the rhombohedral structure is shown in Fig. 6(b). Comparing the TEM images in Figs. 5 and 6 suggests that the Li[$Ni_{0.5}Mn_{0.5}$]O_2 powder underwent a substantial change in the particle morphology while the initial

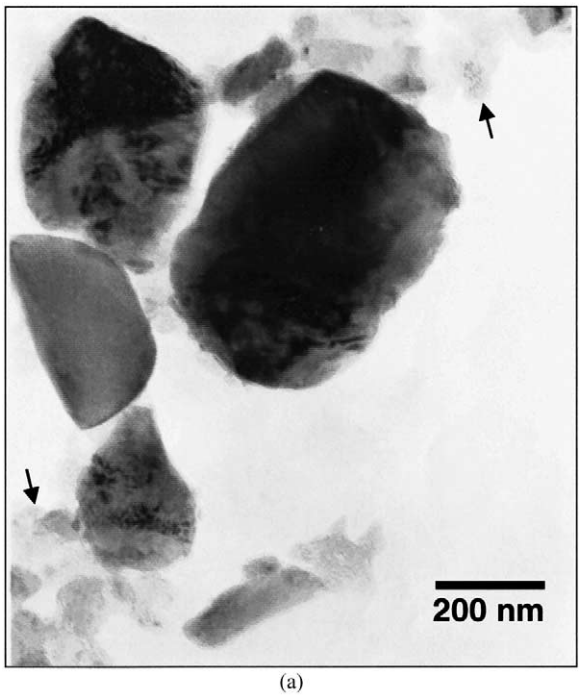

(a)

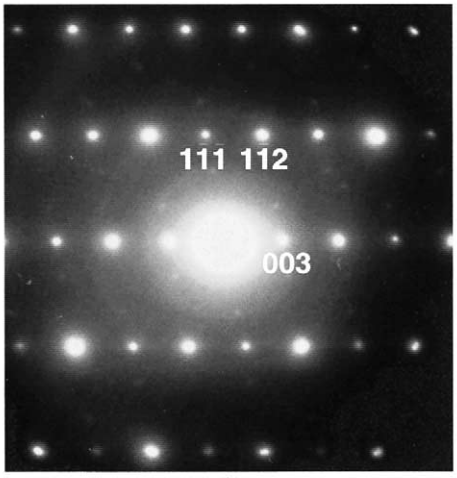

(b)

Fig. 6. (a) Bright field TEM image of the $Li[Ni_{0.5}Mn_{0.5}]O_2$ electrode cycled between 2.8 and 4.3 V (arrows indicate the binder phase which was confirmed using selected area diffraction and energy dispersive spectroscopy); (b) electron diffraction pattern from the cycled particle in 110 zone of the rhombohedral structure.

layered structure was well retained during cycling in spite of the particle agglomeration and growth.

Although it is not clear how the as-prepared powders grew in size, the TEM analysis clearly showed that the $Li[Ni_{0.5}Mn_{0.5}]O_2$ powders prepared by solid-state reaction method went through a major morphological change, without altering its initial layered structure during cycling. Unlike the previous result on the similar material prepared through a different route, our cathode material also well maintained its discharge capacity in spite of the observed morphological change during cycling.

4. Conclusions

We demonstrated that solid-state reaction method can be used to synthesize well-crystallized and uniformly sized $Li[Ni_{0.5}Mn_{0.5}]O_2$ powders. The prepared cathode well maintained its high discharge capacity of 152 mA h g^{-1} in spite of the morphological alteration experienced during cycling from 2.6 to 4.3 V.

Acknowledgements

This work was supported by Korea Science and Engineering Foundation via Research Center for Energy Conversion and Storage and also performed by the financial support of ‘Center for Nanostructured Materials Technology’ under ‘21st Century Frontier R&D Programs’ of the Ministry of Science and Technology, Korea.

References

[1] T. Ohzuka, M. Kitagawa, T. Hirai, J. Electrochem. Soc. 137 (1990) 769.
[2] Y.-K. Sun, Y.-S. Jeon, J. Mater. Chem. 9 (1999) 3147.
[3] K. Amine, H. Tukamoto, H. Yasuda, Y. Fujita, J. Electrochem. Soc. 143 (1996) 1607.
[4] G.G. Amatucci, C.N. Schmutz, A. Bylr, C. Siala, A.S. Gozdz, D. Larcher, J.-M. Tarascon, J. Power Sources 69 (1997) 11.
[5] Y.-K. Sun, D.-W. Kim, Y.-M. Choi, J. Power Sources 79 (1999) 231.
[6] A. Hirano, R. Kanno, Y. Kawamoto, Y. Takeda, K. Yamamura, M. Takano, K. Ohyama, M. Ohashi, Y. Yamaguchi, Solid State Ionics 78 (1995) 123.
[7] A.R. Armstrong, P.G. Bruce, Nature 381 (1996) 499.
[8] G. Vitins, K. West, J. Electrochem. Soc. 144 (1997) 2587.
[9] I.J. Davidson, R.J. Mcllan, J.J. Murray, J.E. Greedan, J. Power Sources 54 (1995) 232.
[10] L. Croguennec, P. Deniard, R. Brec, J. Electrochem. Soc. 144 (1997) 3323.
[11] Y.-I. Jang, B. Huang, Y.-M. Chiang, D.R. Sadoway, Electrochem. Solid-State Lett. 1 (1998) 13.
[12] T. Ohzuku, Y. Makimura, Chem. Lett. (2001) 744.
[13] Z. Lu, D.D. MacNeil, J.R. Dahn, Electrochem. Solid-State Lett. 4 (2001) A191.